
# NAVAL POSTGRADUATE SCHOOL

**MONTEREY, CALIFORNIA**

# THESIS

**DEVELOPING AND TESTING SINTERED AND POLYMER-INFUSED 3D-PRINTED ALUMINUM REACTIVE MATERIALS**

by

Miguel K. Lewis

December 2018

Thesis Advisor: Joseph P. Hooper
Second Reader: Troy Ansell

THIS PAGE INTENTIONALLY LEFT BLANK

| REPORT DOCUMENTATION PAGE | | | *Form Approved OMB No. 0704-0188* |
|---|---|---|---|



| **1. AGENCY USE ONLY** *(Leave blank)* | **2. REPORT DATE** December 2018 | **3. REPORT TYPE AND DATES COVERED** Master's thesis |
|---|---|---|

| **4. TITLE AND SUBTITLE** DEVELOPING AND TESTING SINTERED AND POLYMER-INFUSED 3D-PRINTED ALUMINUM REACTIVE MATERIALS | **5. FUNDING NUMBERS** RPLP7 |
|---|---|
| **6. AUTHOR(S)** Miguel K. Lewis | |
| **7. PERFORMING ORGANIZATION NAME(S) AND ADDRESS(ES)** Naval Postgraduate School Monterey, CA 93943-5000 | **8. PERFORMING ORGANIZATION REPORT NUMBER** |
| **9. SPONSORING / MONITORING AGENCY NAME(S) AND ADDRESS(ES)** N/A | **10. SPONSORING / MONITORING AGENCY REPORT NUMBER** |

**11. SUPPLEMENTARY NOTES** The views expressed in this thesis are those of the author and do not reflect the official policy or position of the Department of Defense or the U.S. Government.

| **12a. DISTRIBUTION / AVAILABILITY STATEMENT** Approved for public release. Distribution is unlimited. | **12b. DISTRIBUTION CODE** A |
|---|---|

**13. ABSTRACT (maximum 200 words)**

Reactive metals (RM) are composites that can augment the lethality of a warhead via the addition of metal combustion. The possibility of producing a viable 3D-printed aluminum RM is considered in this work. Gas-atomized Al powder was used in a binder jet printer to produce green bodies for testing; the porosity of the as-printed materials is on the order of 47%. Sintering of pure Al parts showed little improvement in material density or survivability. Techniques known in the literature to improve Al sintering (addition of tin and use of a reducing atmosphere) were also unsuccessful in giving the parts sufficient strength. Two promising avenues were found. The first is use of gas-atomized aluminum-silicon alloys, which reduces the powder melting point and shows promise for densification of the samples. The second is infusion of the pores with polyurea, which gives the material sufficient strength for use in enhanced blast or incendiary warheads.

| **14. SUBJECT TERMS** reactive materials, additive manufacturing, 3D printing, aluminum, polymer infusion, polymer, sintering | **15. NUMBER OF PAGES** 69 |
|---|---|
| | **16. PRICE CODE** |

| **17. SECURITY CLASSIFICATION OF REPORT** | **18. SECURITY CLASSIFICATION OF THIS PAGE** | **19. SECURITY CLASSIFICATION OF ABSTRACT** | **20. LIMITATION OF ABSTRACT** |
|---|---|---|---|
| Unclassified | Unclassified | Unclassified | UU |

NSN 7540-01-280-5500 Standard Form 298 (Rev. 2-89) Prescribed by ANSI Std. 239-18

THIS PAGE INTENTIONALLY LEFT BLANK

**Approved for public release. Distribution is unlimited.**

# DEVELOPING AND TESTING SINTERED AND POLYMER-INFUSED 3D-PRINTED ALUMINUM REACTIVE MATERIALS

Miguel K. Lewis
Lieutenant, United States Navy
BE, Auburn University, 2010
MA, University of Michigan, 2016

Submitted in partial fulfillment of the
requirements for the degree of

**MASTER OF SCIENCE IN MECHANICAL ENGINEERING**

from the

**NAVAL POSTGRADUATE SCHOOL**
**December 2018**

Approved by: Joseph P. Hooper
Advisor

Troy Ansell
Second Reader

Garth V. Hobson
Chair, Department of Mechanical and Aerospace Engineering

THIS PAGE INTENTIONALLY LEFT BLANK

# ABSTRACT

Reactive metals (RM) are composites that can augment the lethality of a warhead via the addition of metal combustion. The possibility of producing a viable 3D-printed aluminum RM is considered in this work. Gas-atomized Al powder was used in a binder jet printer to produce green bodies for testing; the porosity of the as-printed materials is on the order of 47%. Sintering of pure Al parts showed little improvement in material density or survivability. Techniques known in the literature to improve Al sintering (addition of tin and use of a reducing atmosphere) were also unsuccessful in giving the parts sufficient strength. Two promising avenues were found. The first is use of gas-atomized aluminum-silicon alloys, which reduces the powder melting point and shows promise for densification of the samples. The second is infusion of the pores with polyurea, which gives the material sufficient strength for use in enhanced blast or incendiary warheads.

THIS PAGE INTENTIONALLY LEFT BLANK

# TABLE OF CONTENTS

# LIST OF FIGURES

# LIST OF TABLES

THIS PAGE INTENTIONALLY LEFT BLANK

# LIST OF ACRONYMS AND ABBREVIATIONS

| | |
|---|---|
| 3D | three-dimensional |
| Al | aluminum |
| C | Celsius |
| CYL | cylinder |
| DTRA | Defense Threat Reduction Agency |
| F | Fahrenheit |
| HDRM | high density reactive material |
| kPa | kilo Pascals |
| L/D | length to diameter |
| LLNL | Lawrence Livermore National Laboratory |
| Mg | Magnesium |
| mm | millimeter |
| NPS | Naval Postgraduate School |
| ONR | Office of Naval Research |
| P-1000 | Versalink Polyurea-1000 |
| psi | pounds per square inch |
| RM | reactive material |
| SEM | Scanning Electron Microscope |
| Si | Silicon |
| SHPB | Split Hopkinson Pressure Bar |
| Sn | Tin |
| SOP | standard operating procedure |
| USN | U.S. Navy |
| XRD | X-Ray Powder Diffraction |

THIS PAGE INTENTIONALLY LEFT BLANK

# ACKNOWLEDGMENTS

The author would like to thank his sponsors who funded the research, Jeff Davis at the Defense Threat Reduction Agency (DTRA) and Chad Stoltz at the Office of Naval Research (ONR). Thank you to Robert Reeves and Garth Egan at Lawrence Livermore National Laboratory for their sample procurement and its steadfast assistance in this thesis. The author would also like to thank the following individuals at Naval Postgraduate School: Dr. Joseph Hooper for his patient direction through instruction with this thesis, Jacob Kline for his help with various equipment and data acquisition, and LT Daniel Kotei for his assistance and friendship. Finally, the author would like to thank his wife, Cassandra, and their two daughters, Caleesi and Chanel, for providing the author guiding principles and loving support during his studies at NPS.

THIS PAGE INTENTIONALLY LEFT BLANK

# I. INTRODUCTION

Improving the lethality of a conventional weapon, especially fragmentation warheads, without drastically increasing the cost of the weapon has been a focal point for the U.S Navy for some time [1]. To accomplish this, the use of High-Density Reactive Materials (HDRM) and reactive materials (RM) has been investigated by the Defense Threat Reduction Agency (DTRA), the Office of Naval Research (ONR), and the Naval Postgraduate School (NPS). HDRMs and RMs provide a mechanism for increased overpressure and energy release beyond that obtained from the detonation of a high explosive (HE) in the warhead [2]. Reactive materials generally require intense dynamic loading to begin combusting; this may come during the explosive launch of the material or during high-velocity impact with a target. These two broad mechanisms for energy release from an RM are sometimes referred to as fine particle reaction (FPR) and impact induced reaction (IIR), respectively [3].

Reactive materials must be structurally rigid, and more importantly, must be able to withstand the impact of the warhead into its intended target. The manufacturing method for most RMs under DoD consideration is similar to current powder metallurgy processes of metals and alloys. This thesis examines the possibility of 3D printing a basic metallic reactive material that can serve a similar function. Pure aluminum was chosen as a prototypical RM that has also found applications in DTRA and Air Force warhead concepts. Aluminum (Al) has a high enthalpy of combustion and is relatively inexpensive to manufacture and handle compared to other combustible metals such as boron, hafnium, magnesium, and so on.

Aluminum presents a challenge, however, in that it is traditionally difficult to sinter. In this thesis a binder jetting technique was utilized, which normally requires considerable sintering after printing to densify the material. Pure aluminum materials composed of micron-scale, gas-atomized powders were found to have extremely poor mechanical properties from a binder jet/sintering process. Addition of tin and magnesium, known in the literature to be a viable route to successfully sinter aluminum powders, were also found to be non-viable for binder jet samples. Two successful avenues were examined in this

thesis as means of obtaining some structural strength; the first relied on infusing a cured polyurea binder, and the second utilized a reduced melting point aluminum-silicon alloy. Density, strength, and survivability under dynamic loading were analyzed to evaluate material properties. Both avenues show promise for practical material fabrication for a variety of RM applications.

# II. EXPERIMENTAL METHODOLOGY

## A. BINDER JETTING

All metal 3D printing was done at Lawrence Livermore National Laboratory (LLNL) via its ExOne M-Lab 3D binder jetting metal printer using spherical powders from Valimet Inc. Binder jetting is a process in which layers of metal powder and liquid binding agent are selectively deposited to form a solid part [4, Fig. 1]. After a layer of metal is deposited, the layer of binding agent provides the bond between neighboring particles of metal. After some time, a part is formed by the layers of powder and binder. These printers can assemble complicated parts in a matter of hours that would be difficult or even impossible to machine via standard methods, making it an exotic and intriguing avenue to pursue in developing RMs. Binder jetting also avoids the high temperatures and potential melting that occurs in laser sintering metal printers; though these effects are not detrimental for pure aluminum, they are not viable for many of the multi-component reactive materials under consideration in the DoD.

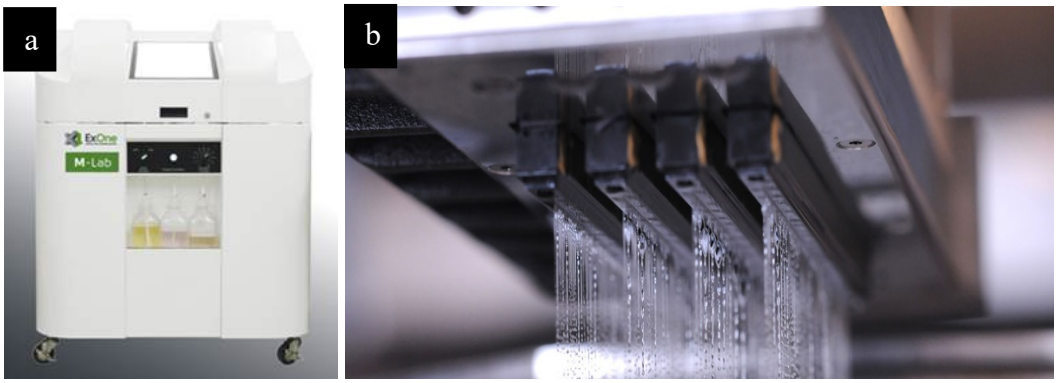


Figure 1. a) ExOne M-Lab 3D Printer. b) Binder addition to powder bed.

The samples used were all the same dimensions in preparation for follow-on testing and research. The samples were 10 mm (0.3937 in) by 10 mm (0.3937 in) cylindrical samples (CYL) as seen in Table 1. Maintaining the length to diameter ratio (L/D) at unity, allows for a myriad of testing and imaging via Split Hopkinson Pressure Bar (SHPB),

Scanning Electron Microscopy (SEM) and Optical Microscope, as well as compositional make-up via X-Ray Powder Diffraction (XRD).

Table 1. AM-103 cylinder dimensions

| Sample # | mass (g) | length (in) | length (mm) | diameter (in) | diameter (mm) | volume (cc) | density (g/cc) | % of Al (2.7g/cc) | Porosity (Pct) | Application |
|---|---|---|---|---|---|---|---|---|---|---|
| 1 | 1.1869 | 0.3980 | 10.1092 | 0.3920 | 9.9568 | 0.7992 | 1.4852 | 55.01% | 44.99% | Polymer |
| 2 | 1.2161 | 0.4217 | 10.7120 | 0.3970 | 10.0850 | 0.9089 | 1.3380 | 49.56% | 50.44% | Sinter |
| 3 | 1.1939 | 0.4057 | 10.3060 | 0.3956 | 10.0470 | 0.8381 | 1.4245 | 52.76% | 47.24% | Sinter |
| 4 | 1.2081 | 0.4195 | 10.6560 | 0.3960 | 10.0590 | 0.8971 | 1.3467 | 49.88% | 50.12% | Sinter |
| 5 | 1.1832 | 0.3949 | 10.0300 | 0.3909 | 9.9300 | 0.7846 | 1.5081 | 55.85% | 44.15% | Polymer |
| 6 | 1.1711 | 0.3949 | 10.0300 | 0.3902 | 9.9100 | 0.7830 | 1.4956 | 55.39% | 44.61% | Polymer |
| 7 | 1.1958 | 0.3947 | 10.0260 | 0.3931 | 9.9850 | 0.7883 | 1.5169 | 56.18% | 43.82% | SHPB |
| 8 | 1.1721 | 0.4044 | 10.2720 | 0.3946 | 10.0220 | 0.8305 | 1.4113 | 52.27% | 47.73% | Polymer |
| 9 | 1.1732 | 0.3989 | 10.1310 | 0.3930 | 9.9830 | 0.8047 | 1.4579 | 53.99% | 46.01% | Polymer |
| 10 | 1.1865 | 0.4022 | 10.2160 | 0.3952 | 10.0380 | 0.8228 | 1.4420 | 53.41% | 46.59% | Polymer |
| 11 | 1.1915 | 0.4072 | 10.3430 | 0.3965 | 10.0720 | 0.8462 | 1.4080 | 52.15% | 47.85% | Polymer |

Table 1 shows the dimensions and properties of the as-printed CYL samples. The green bodies produced by the initial printing are not machinable, so small variations in sizes are seen. A small fraction of samples contained minor imperfections such as layer decomposition or shape irregularity, likely due to shipping, but had negligible effects on testing. The porosity of the green bodies is extremely high, as expected of a binder jet process. As shown in Table 1, regardless of shape or dimension the printed parts have a porosity of 44% - 50%. This is an enormous porosity compared to the traditional powder metallurgy methods used to produce RMs and would traditionally be reduced by a sintering process. However, as mentioned previously aluminum and other common combustible metals used in RM can be challenging to sinter. In this thesis we discuss multiple methods for dealing with this high porosity to produce materials which are still viable for warhead applications.


Figure 2. ExOne Printed Cylinder from LLNL

### 1. Aluminum Powder

The original powder used was that of pure spherical aluminum (99.7% by weight) produced by Valimet [5]. This aluminum is typical of that found in a variety of thermobaric and reactive material warheads. The Valimet powder was of one size, H-15, having a mean particle diameter of roughly 20 μm (0.00078 in), with up to 10% at 40 μm (0.00157 in) and up to 10% at 9 μm (0.00035 in) size particles. Initial tests were conducted on pure aluminum samples, which, as expected, sintered poorly. Additional printings of H-15 aluminum along with small quantities as tin were also done, due to prior research [6, 7] that showed successful densification of aluminum with these inclusions.

### 2. Tin

Based on the lack of sintering of pure aluminum powdered samples, adding tin (Sn) to samples became another course of action to assist the sintering process. The expectation was that the Sn, due to its low melting temperature, would melt in and around the highly porous samples, providing a bond between Al powder particles.

### 3. AM-103

The alloy used most commonly for final samples in this thesis is Additive Manufacturing 103, or AM-103, also procured via Valimet Inc. This powder is specifically designed for maximum density and optimization of mechanical properties makes this a good choice for sintering purposes and wax infill [5]. The powder's composition, Table 2, tends to have better sintering capabilities than pure aluminum due to the additives in the

powder, mainly Silicon (Si). It is postulated that Al and Si, at temperatures near the eutectic, begin to form Al-Si alloys, such as Al4047 that form the backbone of a 3D-printed sample (Fig. 3).

Table 2. AM-103 composition

| | AM-103 (AlSi10Mg) |
|---|---|
| Aluminum | Balance |
| Copper, wt. % | 0.03 Max. |
| Iron, wt. % | 0.40 Max. |
| Magnesium, wt. % | 0.25-0.45 |
| Manganese, wt. % | 0.15 Max. |
| Silicon, wt. % | 9.0-11.0 |
| Titanium, wt. % | 0.15 Max. |
| Zinc, wt. % | 0.10 Max. |
| Other, Each wt. % | <0.05 |
| Other, Total wt. % | <0.15 |

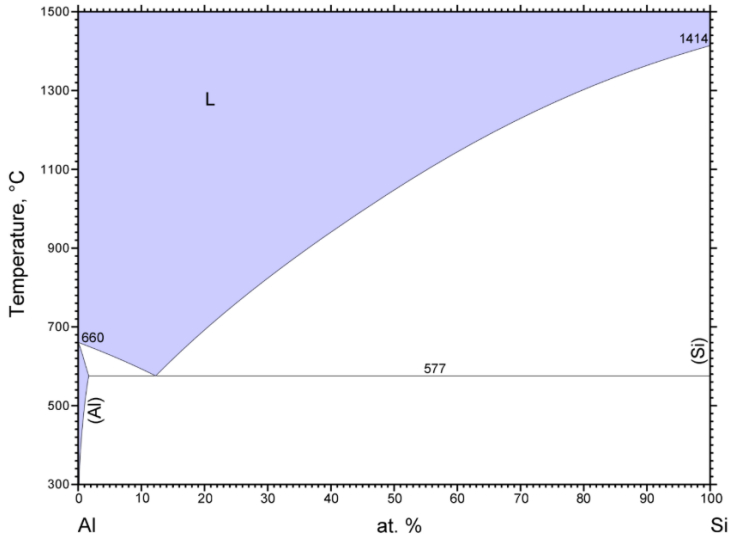


Figure 3. Al-Si Binary Phase Diagram. Image from ASMInternational at https://matdata.asminternational.org/apd/img_image.aspx?dbKey=grantami_apd&id=10710760&revision=398007&height=-1

## B. POLYMER INFUSION

A two-part polyurea mixture was utilized based on favorable results from Schaaf and Nasser [8] in terms of hardening effects and blast mitigation. The mixture included Versalink P-1000 (P-1000) as the prepolymer and Isonate 143L as the cross-linking agent. The P-1000, in this case, serves as the difunctional amine and the Isonate as the hardening agent. Once mixed, the polymer becomes lightly cross-linked and can provide structural support to the sample if properly infused into the porous network.

Polyethylene glycol 3350 and paraffin wax were also experimented with as infusing materials to provide some basic strength. Both infuse readily, and similar wax/Al compounds have been the subject of recent study from a number of DoD organizations. However, for final testing the decision was made to focus on the P-1000 due to its higher strength and toughness after curing.

### 1. Versalink P-1000

Versalink Polyurea-1000 is a polyamine, or oligomeric diamine, and was chosen over polyethylene glycol 3350 (PEG-3350) and paraffin because of P-1000's ease of processing and handling at ambient temperatures and its cross-linking ability. This makes it a perfect candidate for infusion, given it will remain in liquid form until the curing agent is added. All three considered polymers are versatile, but P-1000 when cured with Isonate 143L provides the best qualitative results for continued evaluation. The chemical structure is seen in Figure 4 and shows the amines at either end of the Isonate 143L, which form a hardened structure wax [8].

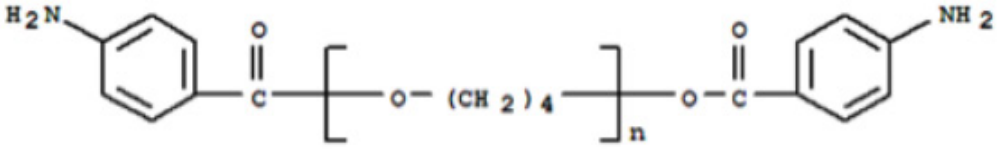


Figure 4. The P-1000 System. Source: [8].

## 2. Isonate 143L

To harden the polymer, Isonate 143L by Dow Chemical was used as a curing agent [8, Fig. 5]. Isonate 143L is a polycarbodiimide-modified diphenylmethane diisocyanate that when combined with a prepolymer, reacts to form a cross-linked structure seen in Figure 6.

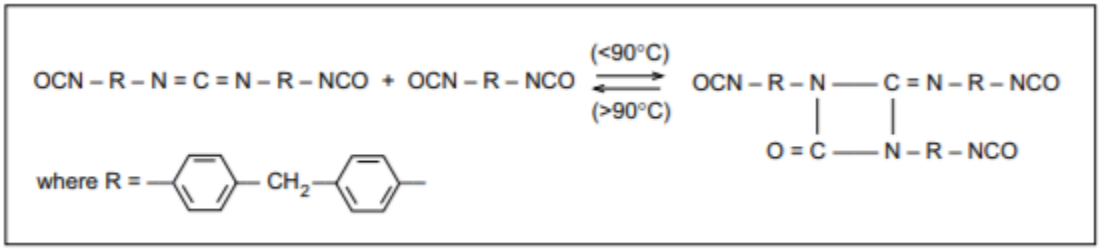


Figure 5. The Isonate 143L System. Source: [8].

The amines in the P-1000 react with the isocyanate groups in the Isonate 143L to form urea linkages. The result is a polyurea, that exhibits 75% of the desired effects within 24 hours and 100% of the effects realized within 14 days [8, Fig. 6]. Although, to accelerate the cross-linking process, heating the polymer at 60°C for 30 min will suffice to reach the desired mechanical properties.

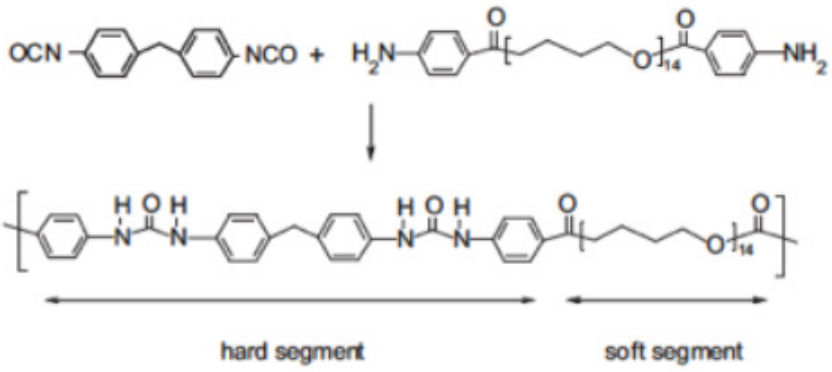


Figure 6. Polyurea: P-1000 and Isonate 143L cross-linked. Source: [8].

### 3. Saturated Sample (Completely Infused)

To infuse the sample cylinder (CYL) with wax, a unique setup was utilized for each group of samples. In this case, the intent was to infuse the CYL with as much P-1000 as possible, which turned out to occupy nearly 100% of the void space in the nominally 40%–50% porous sample. To do this, the CYL was placed in a bath of P-1000 heated in a crucible to 60°C (140°F) to decrease its viscosity and increase the rate of up-take (Fig. 7).

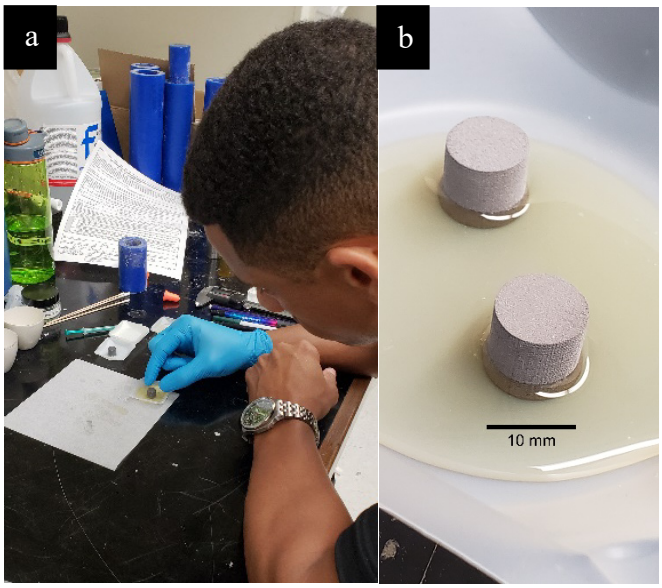


Figure 7. a) Placing sample CYL in P-1000 bath. b) Two sample CYL up-taking in P-1000 bath.

The up-take of P-1000 is approximately 1 mm/min or less, given the standard porosity of AM-103 samples shown in Table 1. This leads to a saturation time for 10 mm (0.3937 in) cylinders of approximately 10–12 min, depending on depth of the P-1000 bath and ambient temperature. Increasing either or both, decreases the up-take time.

Once saturated, the sample is ready for cross-linking. The CYL is coated with 0.2 mL (0.0067 fl. oz.) of Isonate 143L applied via syringe which quickly begins to react with the P-1000 amines to form a solid wax that gives the CYL samples its strength and some ductility as compared to its original brittle state. The curative's isocyanate group interact

with amines in the prepolymer to form a polyurea linkage resulting in after approximately 24 hours a more robust, wax infused 3D-printed metal.

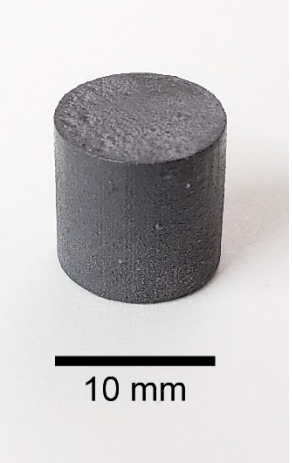


Figure 8. P-1000 infused CYL

#### 4. Coated Sample

Instead of saturating the CYL, a coating of the wax would create a core shell of untouched powder in the center, which might increase the fine particle reaction (FPR) of the RM. To do this, the sample is simply coated with P-1000 and immediately removed from the bath. Given no more than one minute, the excess P-1000 that has not soaked in the CYL was removed via weighing paper to minimize contamination. Immediately thereafter, Isonate 143L was coated on the sample, allowing for another minute of up-take, and, again, wiping the excess clean. This structure will exhibit a hard shell with relatively soft, 3D print interior.

## C. SINTERING OPERATIONS

When the samples are printed they exhibit little to no structural strength, making even basic handling a concern. Binder jet samples are traditionally sintered to burn away binder material and provide some strength via sintering. All heat treatments in this thesis utilized an Across International 1200°C (2192°F) Controlled Atmosphere Muffle Furnace

(Fig. 9) with an inert atmosphere, usually Argon or forming gas (95% Nitrogen/5% Hydrogen). Furnace setup and operation can be found in Appendix A.

Figure 9. Across International Muffle Furnace used for sintering operations

Once an atmosphere and a heat treatment were decided upon, the furnace chamber was purged and filled multiple times to minimize the oxygen content. The native oxide layer in aluminum powders already represents a significant barrier to sintering, and an air-free heat treatment is essential.

## D. HOPKINSON BAR

The cylinders were subjected to dynamic mechanical testing to examine their strength under rapid compressive loading. Such tests provide initial evidence of the survivability of 3D-printed RM parts during explosive/gun launch, penetration, or other common warhead loading scenarios. The NPS split Hopkinson pressure bar in Figure 10 was used for dynamic strength determination. The configuration was standardized for uniform comparisons between the samples. All samples were tested at the same gun pressure with the same aluminum striker, incident, transmission bars.

All tests utilized 19.05 mm (0.75 in) aluminum 6061 bars with an integrated momentum trap. The striker bar was fired using 206.8 kPa (30 psi) of compressed air in

the gas gun. A standard copper pulse shaper 0.53 mm (0.0208 in) thick between the striker and incident bars was used for all shots. Strain gauges on the incident and transmission bars were used to obtain compressive stress/strain curves, and high-speed videography on a Phantom v2512 was used for qualitative analysis of compression and failure.

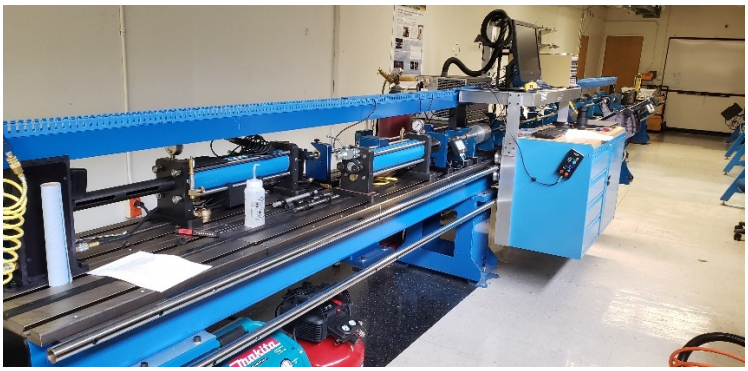

Figure 10. NPS Split Hopkinson pressure bar

## E. INSTRON

Quasi-static compressive data was taken on the Instron 5982 system shown in Figure 11. Due to the low strength of many samples, only two final datasets are presented here, both coated with P-1000 and Isonate 143L. One test was taken at a compression rate of 1 mm/sec (0.0393 in/sec) and one at 0.5 mm/sec (0.0197 in/sec).


Figure 11. NPS Instron 5982 used for quasi-static testing

## F. LIGHT GAS GUN

To determine the possibility of survivability at higher speeds, the light gas gun was utilized. Samples were sabot-launched into 1.5875 mm (0.0625 in) aluminum 2024 plates; this manner of impact has served as a standard to evaluate the fragmentation of reactive materials for several years [9]. Samples were launched at a velocity of 517 m/s (1696.19 ft/sec), 519 m/s (1702.76 ft/sec) and 519 m/s (1702.76 ft/sec), respectively. All failed to perforate at this velocity.

## G. SOUND SPEED TESTING

Sound speed analysis using a pulse-echo technique was used to characterize longitudinal and shear wave speeds and estimate the elastic moduli. Discs of 35 mm (1.378 in) diameter and 2.32 mm (0.0913 in) thickness were used with a standard setup for determining wave speeds. However, due to the high porosity and inclusion of polymer components, a reliable echo was not obtained for any samples discussed here.

# III. RESULTS AND DISCUSSION

## A. PURE ALUMINUM MATERIALS

The average porosity of green bodies produced by binder jet printing of pure H-10 aluminum samples was 46.69%. Though aluminum is known to be challenging to sinter, use as a reactive material does not require full densification or the strength of a traditional forged metal. Thus, a number of sintering schedules were examined for pure aluminum to see if some sintering effects could be obtained despite the large porosity, sufficient for a pure aluminum printed sample to serve as an RM (albeit a very brittle one). Table 3 lists the sintering conditions tested for pure aluminum.

Table 3. Sintered 3D-printed Al samples

| Date | Sample # | Powder | Atmosphere | Heat Up Rate (°C/hr) | Temp. (°C) | Dwell Time (hrs) | Notes |
|---|---|---|---|---|---|---|---|
| 7-Apr | 1 | H-10 Al | Argon | 200 | 627 | 4 | Turns to powder upon handling |
| 12-Apr | 2 | H-10 Al | Argon | 200 | 647 | 8 | Turns to powder upon handling |
| 27-Apr | 3 | H-10 Al | Argon | 200 | 647 | 24 | Turns to powder upon handling |
| 2-May | 4 | H-10 Al | Argon | 200 | 680 | 24 | Able to be handled, yet brittle |
| 15-May | 5 | H-10 Al | Argon | 200 | 725 | 4 | Able to be handled, yet brittle |
| 17-May | 6 | H-10 Al | Argon | 250 | 760 | 4 | Turns to powder upon handling, bluish hue |

### 1. Pure Aluminum

The pure aluminum samples show some evidence of true sintering, but the extent of sintering is insufficient even when the entire material is brought above the aluminum melting point. All post-sintering samples were extremely brittle, due to volatilization of the residual binder and the lack of significant mass diffusion between aluminum powder. As seen in Figure 12.a and 12.b, samples were brittle even to manual handling.


Figure 12. Sintered 3D-printed samples of H-10 aluminum. a) Sample 6 (760°C {1400°F} for 4 hours) b) Sample 2 (647°C {1196.6°F} for 8 hours)

Images of the powders were analyzed under the Scanning Electron Microscope (SEM) and shown in Figure 13.a–c. Some sintering bridges between particles are observed, but they are not sufficiently widespread in the sample to create meaningful material strength.

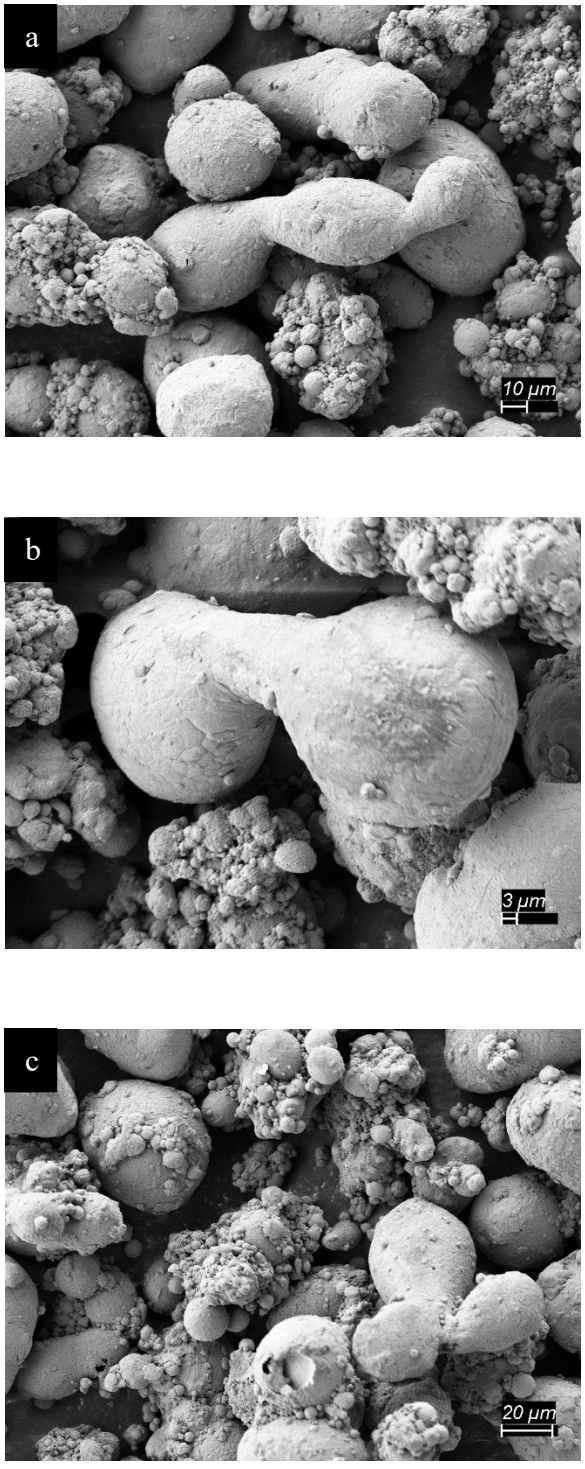


Figure 13. SEM images of sintered 3D-printed samples of H-10 aluminum powder. a) Sintered at 680°C (1256°F) for 24 hours. b) Sintered at 725°C (1337°F) for 4 hours. c) Sintered at 647°C (1196.6°F) for 8 hours.

Several factors contribute to the difficulty in sintering. First, the extremely high porosity of the green body means there is limited intimate contact between the aluminum particles. Second, the high melting point of the aluminum oxide layer on all particles is known to provide a significant barrier to traditional sintering [10]. The binder used in the printer system may serve as another hindrance; at the temperatures shown in Table 3 the binder would be expected to mostly volatilize, but residual carbon or carburization of the aluminum may further limit mass diffusion of the metal. The exact binder chemical makeup is unclear as it is proprietary information [4].

## 2. Methods to Improve Sintering

In order to improve results for pure aluminum, methods known from the aluminum powder metallurgy community were examined. Addition of magnesium, tin, and the use of reducing atmospheres in the sintering furnace had all been shown in the literature to improve sintering results for pure Al [6, 7].

### *a. Tin*

The addition of tin as a liquid phase sintering agent was also considered. A series of materials were printed with a powder mixture of 5 wt.% and the remainder H-10 Al was examined. Using 5 wt.% of Sn did not provide this phenomenon. Tin, with its extremely low melting point, had previously been used to assist in densification of pure aluminum powders formed via traditional metallurgy methods. However, here the results were mixed. The sintering conditions considered are listed in Table 4. The high porosity appeared to allow considerable amounts of tin to exude from the sample, as shown in Figure 14. While there is some minimal strengthening, there is little reduction in porosity at these fractions of tin. Higher concentrations of Sn would improve this but would also add considerable inert material to the final compound which provides no addition of combustion energy.

Table 4. Sintered 3D-printed Al-Sn samples

| Date | Sample # | Powder | Atmosphere | Heat Up Rate (°C/hr) | Temp. (°C) | Dwell Time (hrs) | Notes |
|---|---|---|---|---|---|---|---|
| 1-Jun | 7 | Al-5Sn | Argon | 200 | 521 | 4 | Turns to powder upon handling |
| 22-Jun | 8 | Al-5Sn | Argon | 200 | 400 | 8 | Turns to powder upon handling |
| 28-Jun | 9 | Al-5Sn | N2/H2 | 250 | 620 | 4 | Exudation evident, rigid CYL |
| 5-Jul | 10 | Al-5Sn | Argon | 200 | 700 | 4 | Exudation evident, rigid CYL |

Figure 14 shows an Al-5Sn sample after heating to 620°C (1148°F) for 4 hours. The exuded material is tin, and some post-sintering separation of the print layers can also be observed.


Figure 14. Al-5Sn sample after 620°C (1148°F) for 4 hours of sintering

### 3. AM-103

The addition of magnesium, tin, and reducing atmospheres had all shown success in traditional powder metallurgy samples but provided little benefit for the high porosities of the 3D-printed parts [7]. Two alternate pathways were thus pursued. The first was the use of an aluminum-silicon alloy powder with a reduced melting point. Valimet's AM-103 powder, which has been used in other similar aluminum printing systems, was utilized. Figure 15 shows an AM-103 sample sintered at 700°C (1292°F) for 3 hours. Though there is exuded material, the samples show some evidence of shrinkage consistent with densification. This densification became evident at lower temperatures as well, precluding the shrinkage. The samples were no longer to brittle to handle and showed signs of enough sintering occurred to provide structural rigidity.

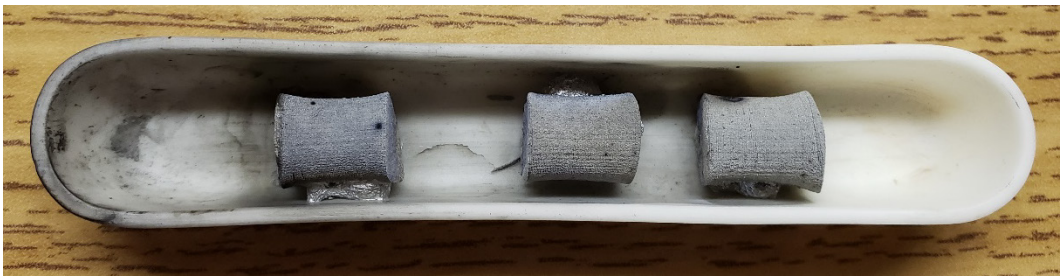

Figure 15. AM-103 Sintered at 700°C (1292°F) for 3 hours

Another sample sintered at a lower temperature (580°C {1076°F} for 2 hours) is shown in Figure 16. This is slightly higher than the eutectic temperature of 577°C (1070.6°F) for Al-Si (Fig. 3). Exudation is observed in the sample, especially around the circumference of the cylinder. However, in contrast to the pure Al samples tested, the AM-103 shows a promising increase in strength and survivability. The tested sintering recipes are shown in Table 5. Further testing and refinement of the sintering table is required to maximize the mechanical properties of the sample.

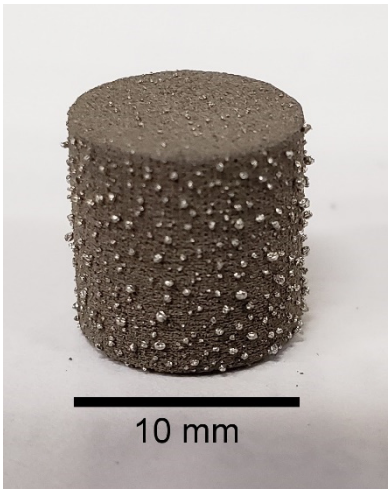


Figure 16. AM-103 Sintered at 580°C (1076°F) for 2 hours

Table 5. Sintered 3D-printed AM-103 samples

| Date | Sample # | Powder | Atmosphere | Heat Up Rate (°C/hr) | Temp. (°C) | Dwell Time (hrs) | Notes |
|---|---|---|---|---|---|---|---|
| 30-Jul | 11 | AM-103 | Argon | 250 | 660 | 2 | Exudation mainly from one location, melted to crucible, structurally robust |
| 5-Oct | 12 | AM-103 | N2/H2 | 250 | 660 | 2 | Exudation mainly from one location, melted to crucible, structurally robust |
| 26-Oct | 13 | AM-103 | Argon | 250 | 580 | 3 | Exudation evident throughout, structurally robust |
| 27-Oct | 14 | AM-103 | Argon | 250 | 700 | 3 | Exudation mainly from one location, melted to crucible, structurally robust |
| 20-Oct | 15 | AM-103 | Argon | 250 | 600 | 2 | Exudation evident throughout, melted to crucible, structurally robust |

## B. POLYMER INFUSION

The second major strategy for producing samples with some mechanical strength was infusing with a polymer. Infusing the green samples, as explained in Ch. 2, was conducted by engulfing samples in a bath of heated P-1000 and combining it with Isonate 143L to allow for cross-linking, which results in a harder and more durable cylinder. The new structure quickly takes on most of the mechanical properties of the polymer. As this strategy is easy to implement and produces materials similar to those under consideration in a number of DTRA RM efforts, the remainder of this thesis focuses on more in-depth analysis of these infused samples.

All saturated samples had an uptake of greater than 92.7% using the method described, calculated using simple density measurements before and after infusion. Figure 17 is an optical microscope image and shows the polymer saturation throughout.

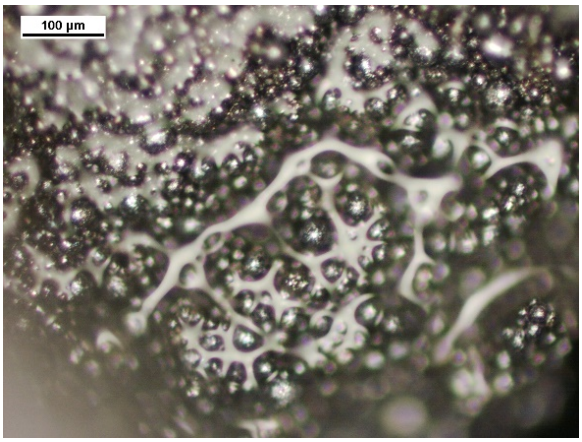


Figure 17. Optical Microscope image of P-1000 infused AM-103 sample surface

### 1. Metal Powders in Infused Samples

As mentioned above, AM-103 continued to be used even for samples where polymer was infused into the void space. It makes for a clear comparison in future studies, especially comparing the sintered to the wax infused samples. Also, choosing AM-103 would result lead to consistent samples for all continued testing. Additionally, lowering the

melt point of the RM may lead to more reactivity if the ignition point of the powders is depressed in a similar way as the melting point [11, 12].

### 2. Material Properties of Infused AM-103

Three polymer systems were analyzed for their uptake into the printed samples; PEG-3350, paraffin wax, and Versalink P-1000 prepolymer. Much of the focus below is on the Versalink systems, as the uptake is rapid, and the cured polymer has improved strength over the other systems. To determine mechanical strength, structural integrity, and dynamic response to impact and loading, the Split Hopkinson Pressure Bar (SHPB) and Instron systems were used.

#### *a. Hopkinson Bar Test Results*

Dynamic compression data is displayed in Figure 18 for samples that were coated and also fully infused with Versalink and Isonate. Tensile testing was not conducted due to the small print sizes available on the ExOne. The average stress each sample was able to withstand was similar, regardless of saturation with P-1000 prior to Isonate 143L addition or if the samples were just coated with P-1000 and subsequent curing agent.

Coating the samples rather than allowing a full infusion does lead to earlier failure as would be expected. This is shown by the drop in stress in Figure 18a past the peak. This method of infusion was chosen for study because maintaining a core shell of effectively just powder could result in more FPR while still having some moderate structural integrity. The average yield stress of coated cylinders was 14.2 MPa (2059.5 psi) (Fig. 18a). The saturated samples, on the other hand, provide a much smoother deformation surface past the peak. With a slightly lower average yield stress at 13.68 MPa (1984.1 psi) (Fig. 18b), the saturated samples hold their shape to considerably higher compression strains.

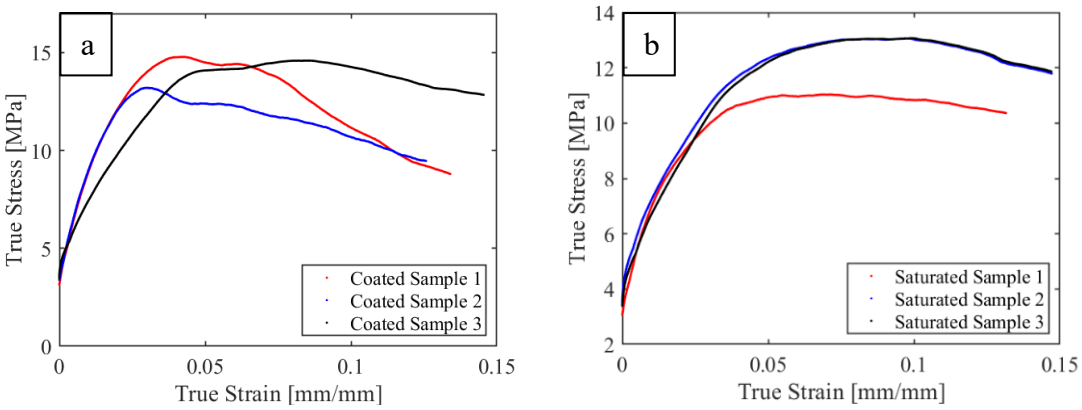


Figure 18. Hopkinson bar stress-strain curves. a) Coated CYL, average strain-rate: 1181.72 $s^{-1}$ b) Completely infused, Average Strain-Rate: 1163.85 $s^{-1}$.

The dynamic stress/strain curve of a pure polyurea sample with no aluminum (Fig. 19) is shown in Figure 20. Two strain rates were analyzed, and the overall strength of the sample is rate-dependent as expected for a polymer. Both samples strained to a deformation of 15% without observable failure. The peak stresses in these tests are comparable to those seen on the filled polyurea materials, suggesting that the aluminum in the printed samples is not adding considerable compressive strength beyond what the pure cured P-1000 provides.

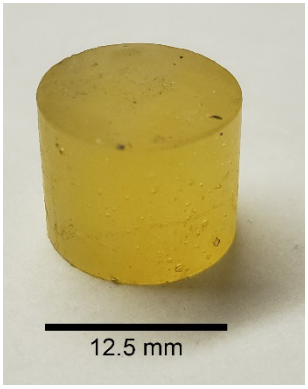


Figure 19. P-1000 and Isonate 143L CYL after SHPB shot

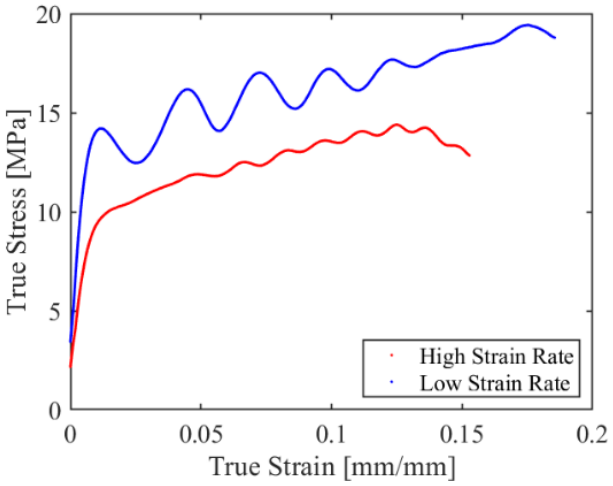


Figure 20. Polymer stress-strain curve at average strain-rates of 1294.13 $s^{-1}$ (low) and 1867.25 $s^{-1}$ (high)

### *b. Instron Quasi-static Test Results*

Quasi-static compression data on Al cylinders infused with P-1000 is shown in Figure 21. A high compression strength was not expected based on previous responses during dynamic testing. At these lower rates, the samples reach a peak stress of 5–7 MPa followed soon after by material failure around 10.5% strain.

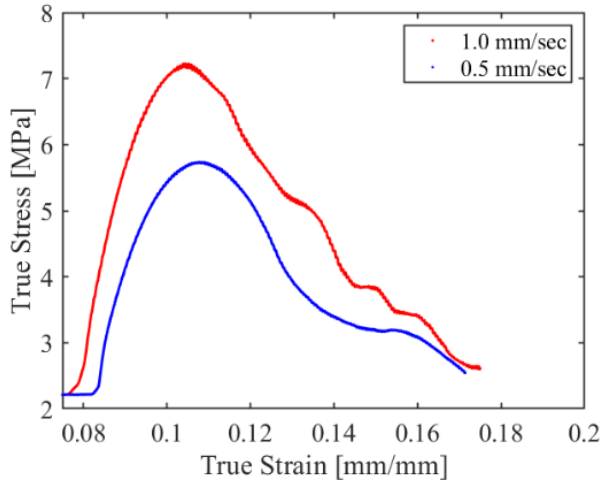


Figure 21. Quasi-static compression of two polyurea-infused printed aluminum cylinders. Two compression rates are shown.

### 3. Infused CYL Strength Assessment

The overall strength of infused samples is relatively low, but this is a favorable quality to have for certain RM applications. If a RM can survive basic handling but breaks up into its powder form during explosive launch, this is optimal for scenarios where combustion near or within the fireball is desired. This is common for enhanced blast and counter-chem/bio warheads Naturally, the low-strength samples here are unsuitable for scenarios where the RM must provide some degree of structural support. The P-1000 and Isonate 143L mixture has a number of advantages over a simple wax infusion. The cured polymer will not melt and has considerable durability in handling. This is advantageous for systems which may undergo thermal cycling in storage.

### 4. Light Gas Gun Shots

As a quick evaluation of survivability, the light gas gun was used to examine impact damage on a polymer infused sample at velocities found in Table 6. The Al2024 impact plate was used to mimic similar tests on other reactive materials conducted at NPS [1, 13]. As seen from the screen captures in Figure 22, the CYL deforms the plate heavily but fails to perforate. Some combustion is observed on impact, and the sample is fragmented catastrophically. Despite the failure to perforate, more damage to the plate was caused than expected (Fig. 23 and Fig. 24). The tests also showed that the material survived drag forces without premature breakup before striking the target.

Table 6. Gas gun shots data

| Sample # | Mass (g) | Impact Velocity (m/s) | Plate Material | Supply Pressure (psi) |
|---|---|---|---|---|
| 1 | 1.4506 | 517.556 | Al2024 | 782.1 |
| 2 | 1.3432 | 519.112 | Al2024 | 868.4 |
| 3 | 1.4067 | 519.883 | Al2024 | 871.8 |

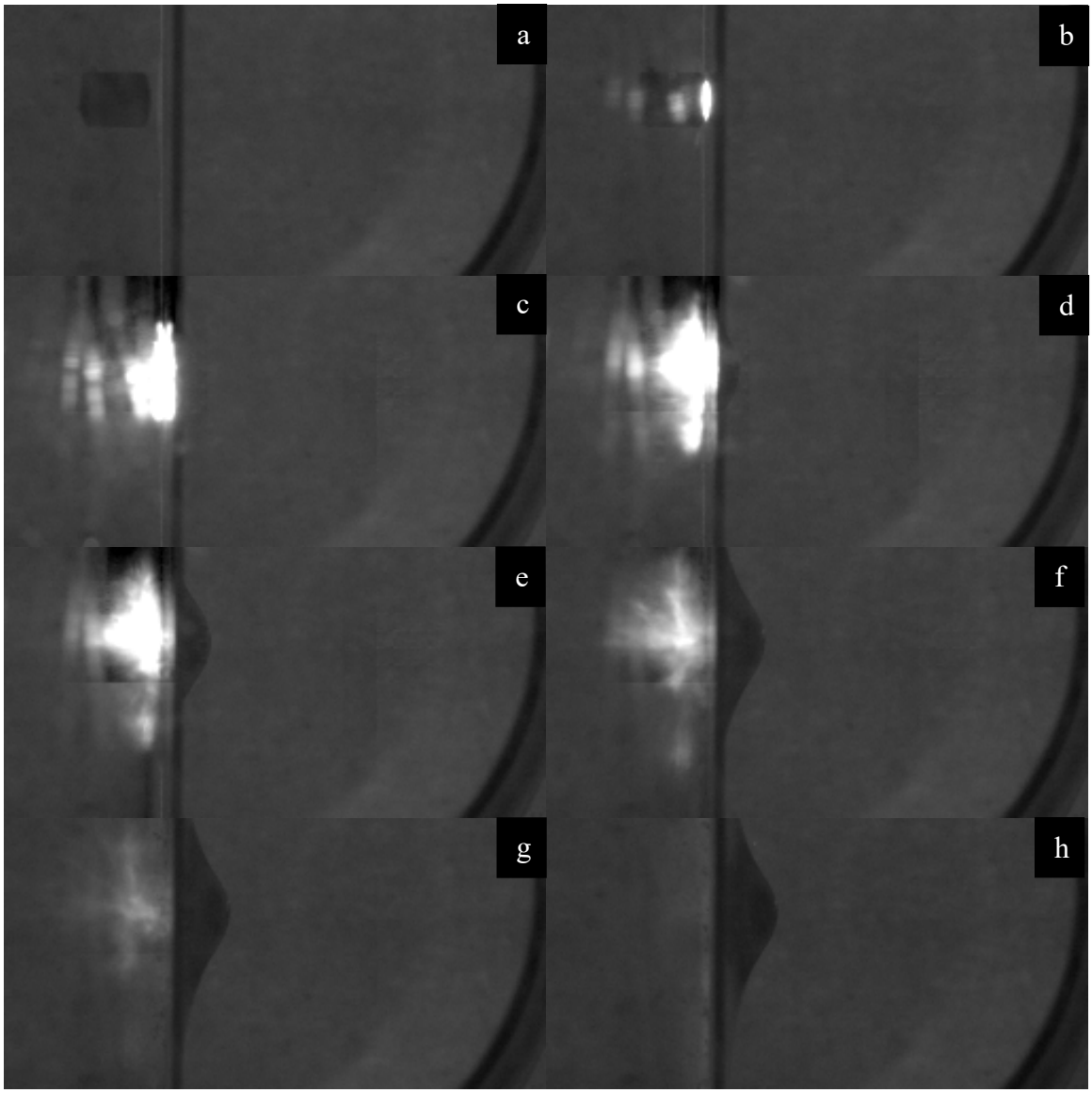


Figure 22. Screen captures from light gas gun shots of infused CYL at Al2024 plate

Figure 22 shows the impact flash and damage associated with impact of the AM-103 infused CYL on the Al2024 plate.


Figure 23. Light gas gun shots. a) Shot #1 perforated the plate. b) Shot #2 was at slight angle upon impact. c) Shot #3 was head on but did not perforate the plate.

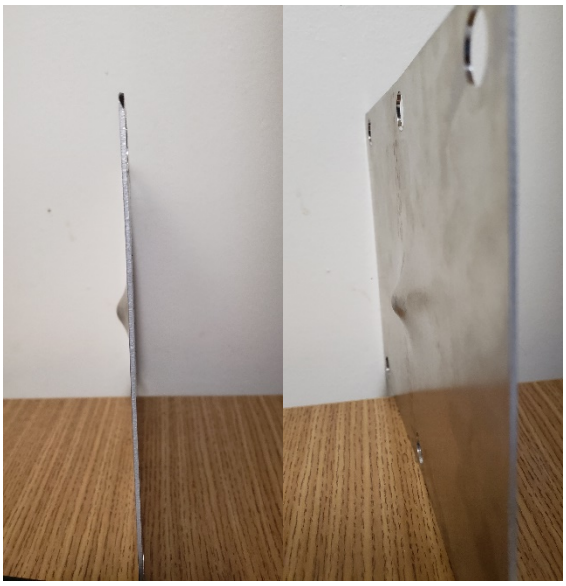

Figure 24. Side views of Al2024 plate from Shot #2

# IV. CONCLUSIONS AND FUTURE WORK

Techniques for producing viable 3D-printed aluminum reactive material samples were explored. The goal was to produce samples with some degree of strength and survivability, but which were still sufficiently brittle to fragment heavily and contribute to warhead lethality via metal combustion. A binder-jet printing system was used along with gas-atomized Al powder to produce samples for heat treatment and mechanical testing. The green bodies produced by the printing have very high porosities, on the order of 47%. As expected, post-printing heat treatments of pure Al samples results in removal of the binder but minimal true sintering of the Al. The native oxide layer of the Al powder, combined with minimal contact between particles in the printed piece, limits the effectiveness of sintering even at temperatures above the Al melting point. Even with aggressive sintering recipes, samples could not survive basic handling.

Several known literature techniques for improving aluminum sintering were attempted for the printed pieces. These included addition of tin (for liquid phase sintering), magnesium (to reduce the oxide layer), and a reducing gas atmosphere. Unlike in traditional Al powder metallurgy, the high starting porosities of the printed green bodies limits the applicability of these techniques and none were found to provide improvements in material strength seen in literature results.

Two promising avenues for viable materials were found. The first is the use of aluminum-silicon alloys, which provides a considerable reduction in the powder melting point. Though additional work is needed to optimize the sintering strategy, these samples show promise for improved strength and densification.

The second strategy involves infusion of a polymeric binder into the printed green body. Due to the high porosities, uptake of waxes or prepolymers is very efficient. Samples infused with a polyurea and then cured were shown to be reasonably robust under dynamic loading, albeit with low strength values compared to pure metallic reactive materials. Hopkinson bar and gas gun impact data on a polyurea/Al composite produced via 3D

printing show that its properties may be suitable for reactive warheads that rely on enhanced blast or incendiary effects for additional lethality.

# APPENDIX A. ACROSS INTERNATIONAL 1200°C MAX CONTROLLED ATMOSPHERE MUFFLE FURNACE SOP

## A1. Required Materials

- Muffle Furnace
- Crucible
- Furnace Door Block
- Tongs
- Thermal Gloves
- Sample

## A2. AI Furnace Operation

1. Open furnace door by loosening all door locks
2. Don thermal gloves
3. Place sample inside crucible in the furnace.

Figure 1: Placing sample in the furnace

4. Place furnace door block inside of furnace door.
    a. NOTE: The door block may have been left out from the last operation, but always needs to be replaced prior to heating operations.

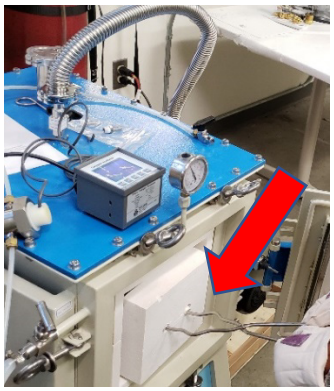

Figure 2: Placing furnace door block in the furnace

5. Doff thermal gloves
6. Close the furnace door lightly and tighten the door locks no more than “finger tight”.
    a. Note: the vacuum on the furnace will “suck” the door tightly shut and possibly cause the door locks to come loose. Retighten door if this happens.
7. Verify all inlets and outlets valves to the furnace are shut.
8. Draw vacuum on the furnace
    a. Start vacuum pump

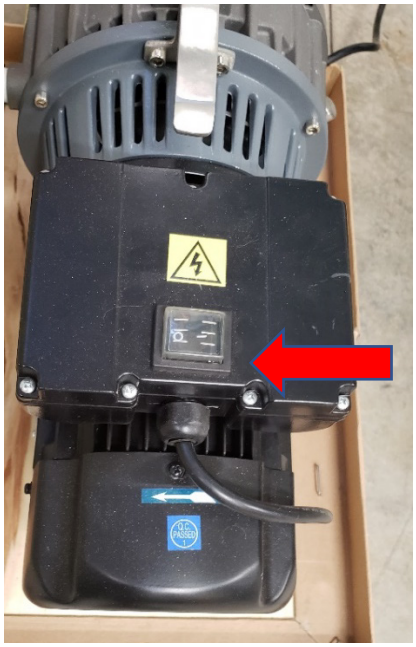

Figure 3: The vacuum pump controls

    b. Open TO PUMP/BURN OUT PORT VALVE on top of furnace

Figure 4: The TO PUMP/BURN OUT PORT VALVE on top of furnace

c. Verify gage pressure decreasing

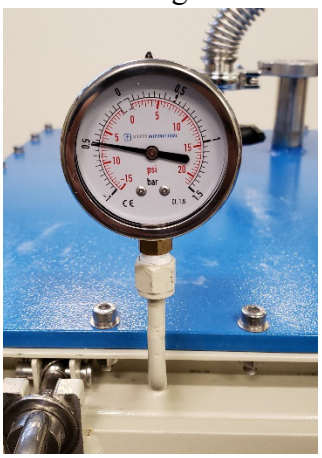

Figure 5: Vacuum/Pressure gauge atop furnace

i. Retighten door locks as necessary

d. Shut burn out port valve when desired vacuum pressure has been attained
e. Stop vacuum pump

9. Fill furnace with Argon / Nitrogen / Helium / Forming gas
   a. Open GAS TANK VALVE

Figure 6: Gas Cylinder regulator

b. Open GAS INLET VALVE at back of furnace

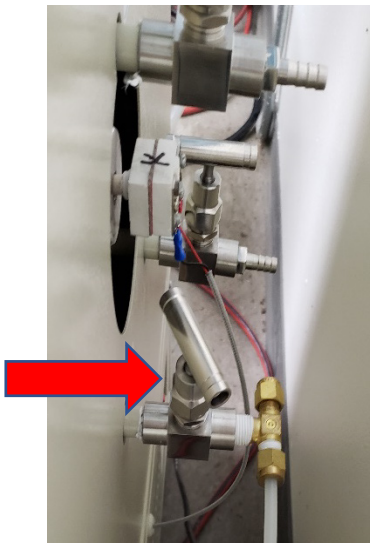

Figure 7: GAS INLET VALVE in back of furnace

c. Open REGULATOR 90-DEGREE VALVE near tank

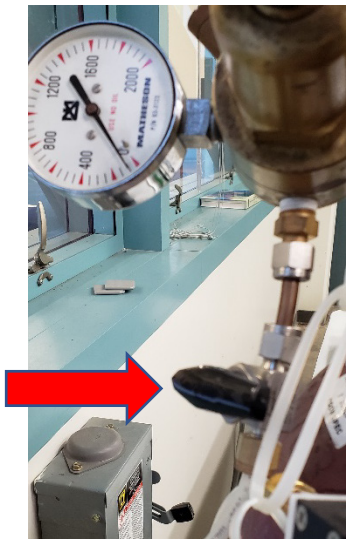


Figure 8: REGULATOR 90-DEGREE VALVE at cylinder

d. Set pressure regulator to desired flow rate
    i. NOTE: No greater than 10 L/min.

Figure 9: Flow meter at cylinder

e. Fill to desired pressure
    i. CAUTION: No greater than **3 psi**. Higher pressures will cause door locks to be damaged.
f. Shut REGULATOR 90-DEGREE VALVE
g. Shut GAS INLET VALVE

10. Repeat steps 5 & 6 at least 3 times to ensure furnace space has been sufficiently evacuated of air.
    a. NOTE: Purging and filling less may cause oxygen to remain in atmosphere.
11. Purge the furnace one last time prior to turning on heating elements to no greater than **-7 psi**. This will ensure the pressure does not reach an excessive value while heating.
    **IMPORTANT**: Heating at positive pressure can result in damage to the equipment and personnel.
12. Place SWITCH in the horizontal position as shown to energize the furnace


Figure 10: Front console of furnace. Switch.

13. Press TURN ON button

a. NOTE: This turns on power to the heating coils
b. NOTE: This button only illuminates if the contact inside the door has been depressed, i.e. the door is firmly shut.

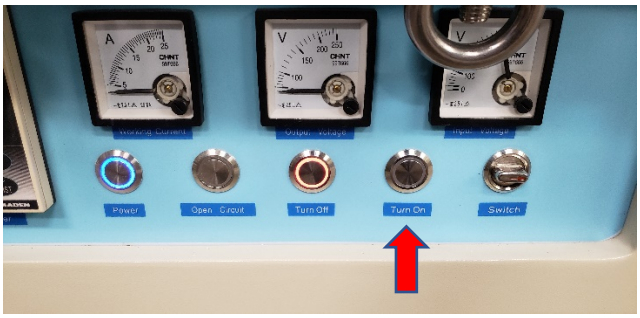


Figure 11: Front console of furnace. Turn On button.

**A3. AI Furnace Software Operation**

1. Log in to computer
2. Open the Shimaden Lite software


Figure 12: Shimaden Lite software

3. Verify COM Mode is selected to COM

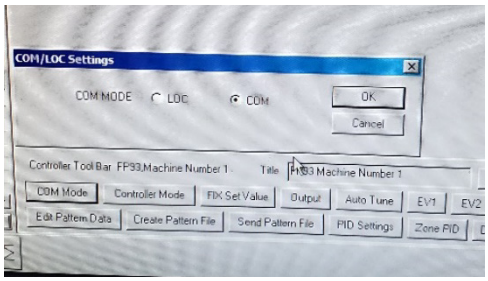


Figure 13: COM/LOC Settings window

4. Set Pattern Parameters by clicking EDIT PATTERN DATA
    a. Edit the Set Value (SV) Temperature
    b. Edit the Time
        i. The time will dictate the heat up rate for the Step 1
        ii. NOTE: A heat up rate greater than 250°C/hr will result in an error.
    c. Verify proper PID is selected (Refer to Operation Manual for PID selection)

d. Repeat steps 4.a – 4.c for all desired steps

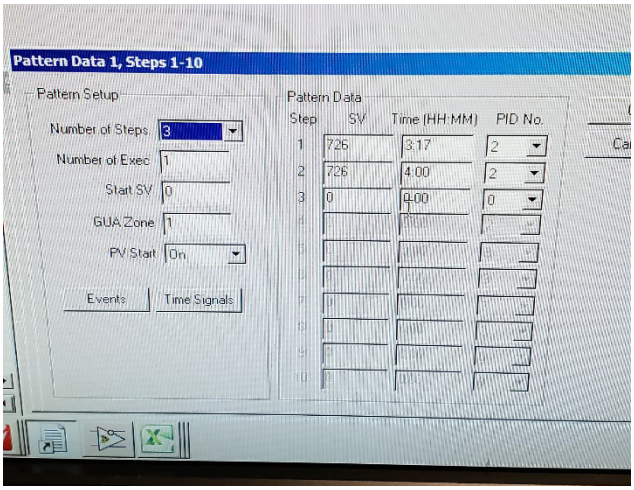

Figure 14: EDIT PATTERN DATA window

5. Start selected pattern by clicking CONTROLLER MODE
    a. Select RUN
    b. NOTE: Once the pattern has completed the furnace will stop and begin to cool to ambient, but not turn off electrically.

**A4. Removing sample from furnace**

1. Once heat treatment is complete, vent the furnace
    a. Press TURN OFF button on furnace
    b. Place SWITCH in vertical position

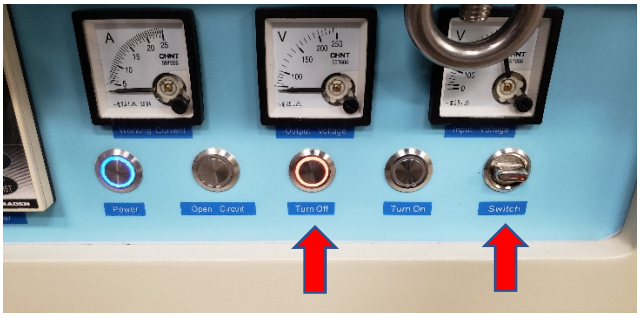

Figure 15: Front console of furnace. Turn Off button and Switch.

c. Open one or both of the furnace GAS VALVES to vent furnace

Figure 16: Both GAS VALVES on the left side of furnace

d. Once the gage returns to **~0 psi**, loosen door locks
e. Open furnace door
   CAUTION: Contents may still be hot.
f. Don thermal gloves
g. Remove door block using tongs
h. Remove sample using tongs
i. Doff thermal gloves

# APPENDIX B. MATLAB CODE

## A. HOPKINSON BAR PLOTS

```
clc
close all
clear
%% Loading SHPB Data
Coat1=xlsread('AM103_P1000_Isonate',2,'U3:X9150'); % Reads data from
Excel file
Coat2=xlsread('AM103_P1000_Isonate',2,'Z3:AC8200');
Coat3=xlsread('AM103_P1000_Isonate',2,'AE3:AH8800');
Sat1=xlsread('AM103_P1000_Isonate',2,'AJ3:AM8580');
Sat2=xlsread('AM103_P1000_Isonate',2,'AO3:AR9580');
Sat3=xlsread('AM103_P1000_Isonate',2,'AT3:AW9580');
Polymer1=xlsread('AM103_P1000_Isonate',2,'AY3:BB9450');
Polymer2=xlsread('AM103_P1000_Isonate',2,'BD3:BG7950');
%% Coated Sample Data
Coat1_time=Coat1(:,1);        % ORDER: (Row/Column)
Coat1_StrainRate=Coat1(:,2);
Coat1_Strain=Coat1(:,3);
Coat1_Stress=Coat1(:,4);
A=smoothdata(Coat1_Stress); % Smooth data to reduce oscillations
Max1=max(A);     % Find maximum in the data

Coat2_time=Coat2(:,1);
Coat2_StrainRate=Coat2(:,2);
Coat2_Strain=Coat2(:,3);
Coat2_Stress=Coat2(:,4);
B=smoothdata(Coat2_Stress);
Max2=max(B);

Coat3_time=Coat3(:,1);
Coat3_StrainRate=Coat3(:,2);
Coat3_Strain=Coat3(:,3);
Coat3_Stress=Coat3(:,4);
C=smoothdata(Coat3_Stress);
Max3=max(C);
Maxes1=[Max1 Max2 Max3];
Stress_avg1=mean(Maxes1)     %Determine the mean stress of coated
samples
%% Plotting Coated Sample Data
plot(Coat1_Strain,A,'.r','MarkerSize',5)
hold on
plot(Coat2_Strain,B,'.b','MarkerSize',5)
hold on
plot(Coat3_Strain,C,'.k','MarkerSize',5)
hold off
xlabel('True Strain [mm/mm]','FontName','Times New
Roman','FontSize',22) ;
ylabel('True Stress [MPa]','FontName','Times New Roman','FontSize',22)
;
```

```
set(gca,'FontName','Times New
Roman','FontSize',16,'box','on','LineWidth',1.1) ;
legend('Coated Sample 1','Coated Sample 2','Coated Sample
3','Location','Southeast')%,'Orientation','horizontal')
axis([0 0.15 0 17]);

%% Saturated Sample Data
Sat1_time=Sat1(:,1);       % ORDER: (Row/Column)
Sat1_StrainRate=Sat1(:,2);
Sat1_Strain=Sat1(:,3);
Sat1_Stress=Sat1(:,4);
D=smoothdata(Sat1_Stress);
Max3=max(D);

Sat2_time=Sat2(:,1);
Sat2_StrainRate=Sat2(:,2);
Sat2_Strain=Sat2(:,3);
Sat2_Stress=Sat2(:,4);
E=smoothdata(Sat2_Stress);
Max3=max(E);

Sat3_time=Sat3(:,1);
Sat3_StrainRate=Sat3(:,2);
Sat3_Strain=Sat3(:,3);
Sat3_Stress=Sat3(:,4);
F=smoothdata(Sat3_Stress);
Max3=max(F);
Maxes2=[Max1 Max2 Max3];
Stress_avg2=mean(Maxes2)
%% Plotting Saturated Sample Data
figure
plot(Sat1_Strain,D,'.r','MarkerSize',5)
hold on
plot(Sat2_Strain,E,'.b','MarkerSize',5)
hold on
plot(Sat3_Strain,F,'.k','MarkerSize',5)
hold off
xlabel('True Strain [mm/mm]','FontName','Times New
Roman','FontSize',22) ;
ylabel('True Stress [MPa]','FontName','Times New Roman','FontSize',22)
;
set(gca,'FontName','Times New
Roman','FontSize',16,'box','on','LineWidth',1.1) ;
legend('Saturated Sample 1','Saturated Sample 2','Saturated Sample
3','Location','Southeast')%,'Orientation','horizontal')
%% Polymer Only Sample Data
Poly1_time=Polymer1(:,1);       % ORDER: (Row/Column)
Poly1_StrainRate=Polymer1(:,2);
Poly1_Strain=Polymer1(:,3);
Poly1_Stress=Polymer1(:,4);
G=smoothdata(Poly1_Stress);

Poly2_time=Polymer2(:,1);
Poly2_StrainRate=Polymer2(:,2);
Poly2_Strain=Polymer2(:,3);
```

```
Poly2_Stress=Polymer2(:,4);
H=smoothdata(Poly2_Stress);
%% Plotting Polymer Sample Data
figure
plot(Poly1_Strain,G,'.r','MarkerSize',5)
hold on
plot(Poly2_Strain,H,'.b','MarkerSize',5)
hold off
xlabel('True Strain [mm/mm]','FontName','Times New
Roman','FontSize',22) ;
ylabel('True Stress [MPa]','FontName','Times New Roman','FontSize',22)
;
set(gca,'FontName','Times New
Roman','FontSize',16,'box','on','LineWidth',1.1) ;
legend('High Strain Rate','Low Strain Rate','Location','Southeast');
```

## B. INSTRON TEST PLOTS

```
clc
close all
clear
%% Loading Instron Data
AM103_1 = xlsread('Instron_1_1','A3:O7213');
%% Coated Sample Data
Strain1 = AM103_1(:,5);       % ORDER: (Row/Column)
Stress1 = AM103_1(:,7);
Strain2 = AM103_1(:,13);
Stress2 = AM103_1(:,15);
%% Plotting Data
plot(Strain1,Stress1,'.r','MarkerSize',5)
hold on
plot(Strain2,Stress2,'.b','MarkerSize',5)
hold off
xlabel('True Strain [mm/mm]','FontName','Times New
Roman','FontSize',22) ;
ylabel('True Stress [MPa]','FontName','Times New Roman','FontSize',22)
;
set(gca,'FontName','Times New
Roman','FontSize',16,'box','on','LineWidth',1.1) ;
legend('1.0 mm/sec','0.5 mm/
sec','Location','Northeast')%,'Orientation','horizontal')
axis([0.075 0.2 2 8]);
```

THIS PAGE INTENTIONALLY LEFT BLANK

# APPENDIX C. SEM IMAGES

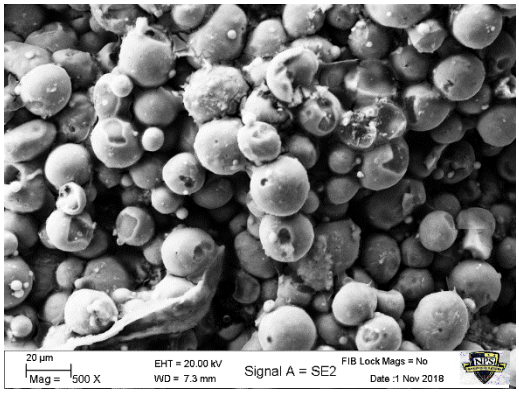


SEM image of AM-103 sintered at 700°C (1292°F) showing some coalescence

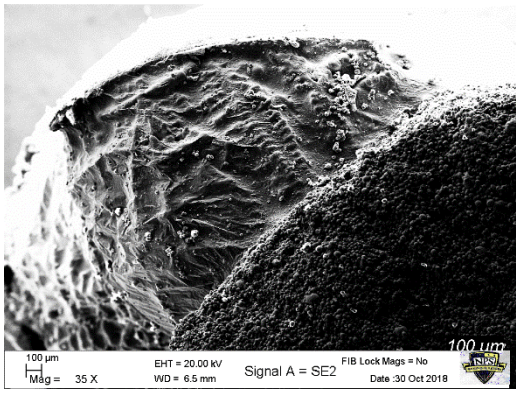


SEM image of AM-103 sintered at 700°C (1292°F) showing exudation from CYL

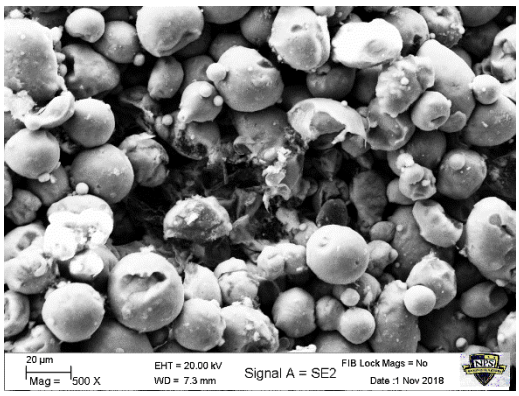


SEM image AM-103 sample sintered at 700°C (1292°F) showing powder coalescence

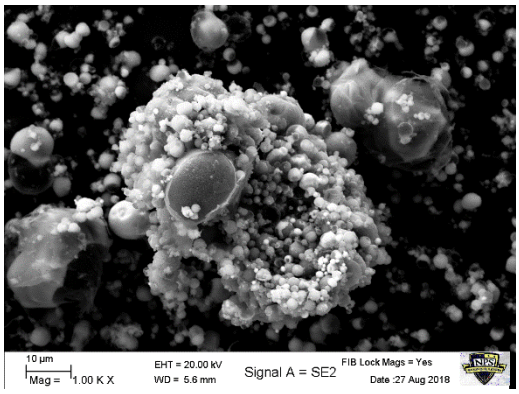

SEM image of AM-103 powder with infused P-1000

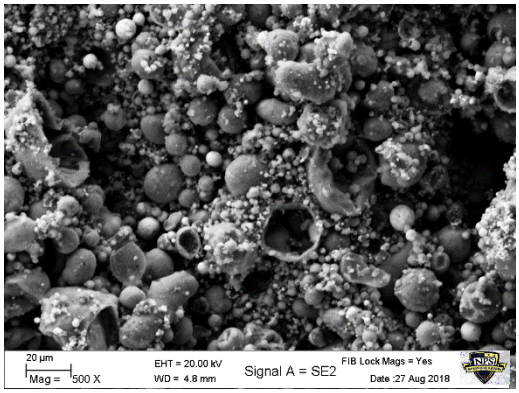

SEM image of AM-103 powder with infused P-1000

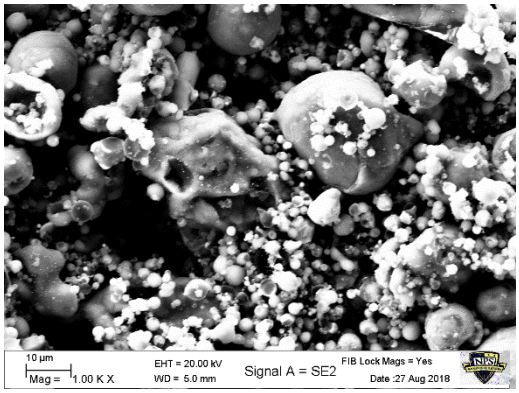

SEM image of AM-103 powder with infused P-1000

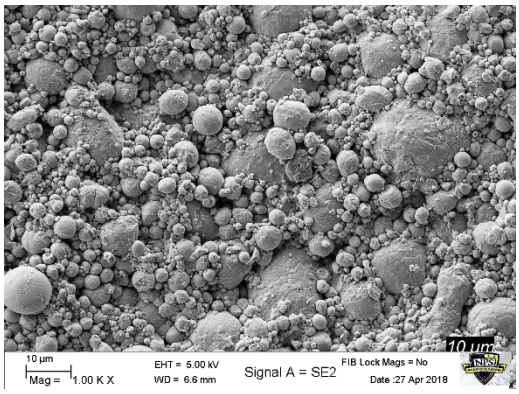

SEM image H-2/H-15 powder as comparison

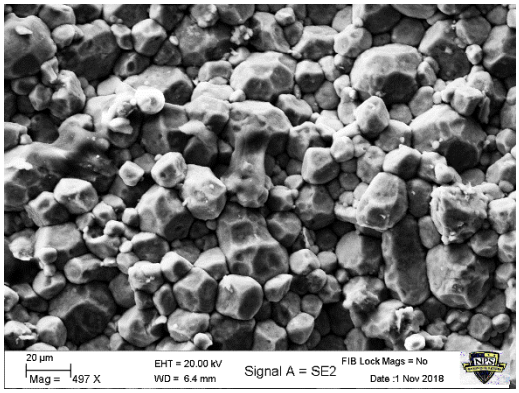

SEM image of H-15 CYL cold isostatically pressed

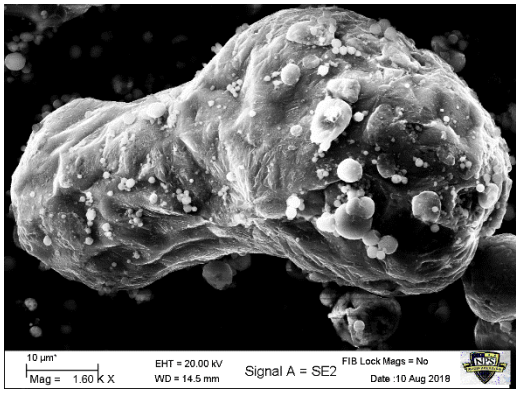

SEM image of Al-Sn sample sinter bridge

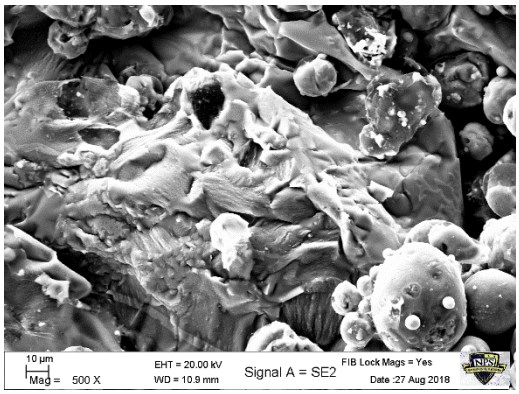

SEM image of Al-Sn sintered sample

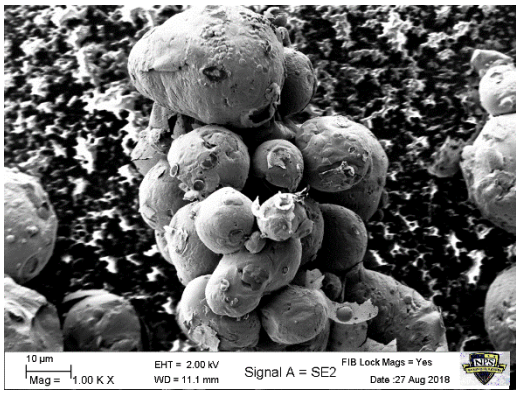

SEM image of Al-Sn sintered sample

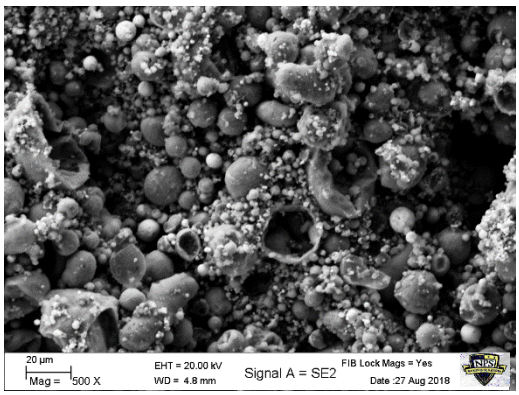

SEM image of AM-103 sintered sample

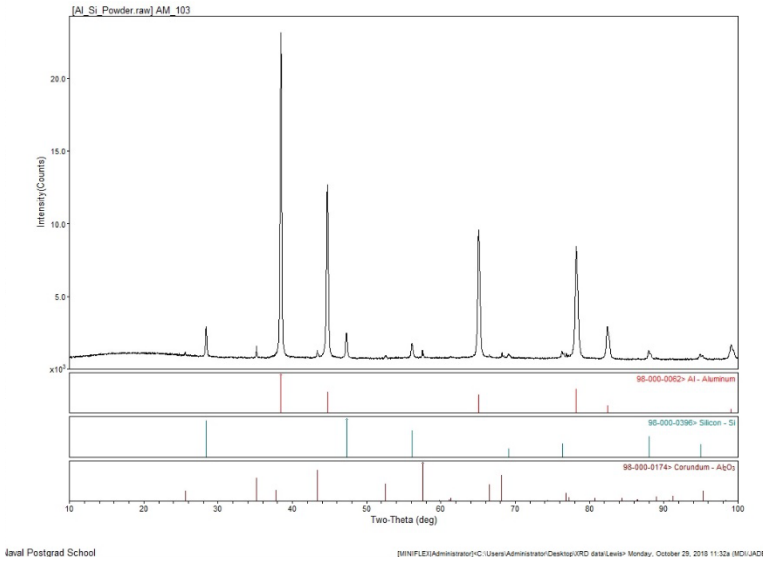


XRD diffraction pattern of sintered AM-103 sample

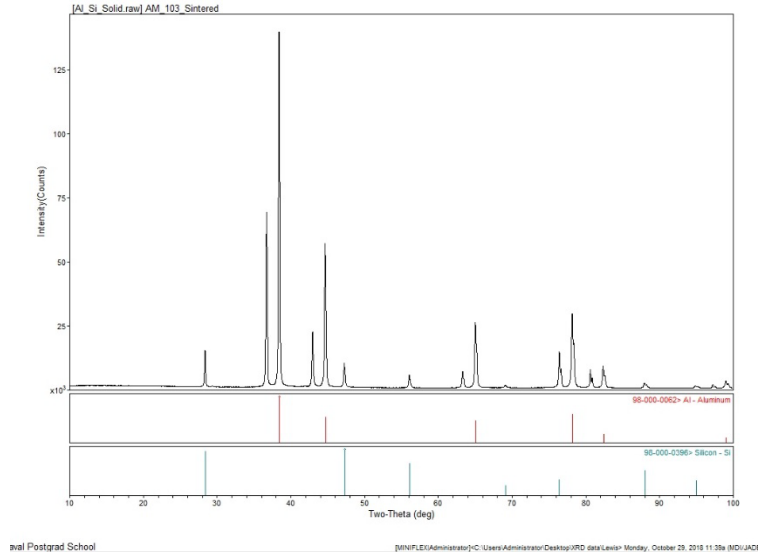


XRD diffraction pattern of sintered AM-103 powder sample

THIS PAGE INTENTIONALLY LEFT BLANK

# LIST OF REFERENCES


[1] S. L. Patrick, "Ballistic and fragmentation of the M7 reactive material against oblique targets," M.S. thesis, Dept. of Physics, NPS, Monterey, CA, USA, 2017.

[2] "Weapons physics," class notes for Terminal Ballistics and Shock Physics, Dept. of Mechanical and Aerospace Engineering, Naval Postgraduate School, Monterey, CA, Apr. 2018.

[3] K. Kim, W. Wilson, "Three different structural reactive material (SRM) casings under explosive loading," *Proc. 24th International Symposium on Military Aspects of Blast and Shock*, Jul. 2015.

[4] ExOne. "What is Binder Jetting?" Accessed March 1, 2018. [Online]. Available: https://www.exone.com/Resources/Technology-Overview/What-is-Binder-Jetting.

[5] Valimet Inc. "Additive Manufacturing," Accessed November 2018. [Online]. Available: http://valimet.com/our-products/am-grades/.

[6] R. N. Lumley, T. B. Sercombe, and G. B. Schaffer, "Surface oxide and the role of magnesium during the sintering of aluminum," Metallurgical and Materials Transactions, vol 30A, Dec. 1999.

[7] I. A. MacAskill, R. L. Hexemer, I. W. Donaldson, and D. P. Bishop, "Effects of magnesium, tin, and nitrogen on the sintering response of aluminum powder," Journal of Materials Processing Technology, Aug. 2010. doi:10.1016/ j.jmatprotec.2010.08.018

[8] K. Schaaf and S. Nemat-Nasser, "Characterization of elastomeric composite materials for blast mitigation," Mechanics of Time-Dependent Materials and Processes in Conventional and Multifunctional Materials, vol. 3, May 2011. doi: 10.1007/978-1-4614-0213-8_19

[9] T. A. Booth-Seay, "Soft catch and fragmentation of Navy reactive materials," M.S. thesis, Dept. of Eng. and App. Sci., NPS, Monterey, CA, USA, 2017.

[10] Z. Y. Liu, T. B. Sercombe, and G.B. Schaffer, "The effect of particle shape on the sintering of aluminum," *Metallurgical and Materials Transactions*, vol. 38A, Jun. 2007. [Online]. Doi:10.1007/s11661-007-9135-2

[11] Y. Aly, M. Schoenitz & E. L. Dreizin, "Aluminum-metal reactive composites," *Combustion Science and Technology*, vol. 183, iss. 10, pp. 1107–1132, Sep. 2011. [Online]. doi:10.1080/00102202.2011.584090

[12] T. R. Sippel, S. F. Son, and L.J. Groven, "Altering reactivity of aluminum with selective inclusion of polytetrafluoroethylene through mechanical activation," *Propellants, Explosives, Pyrotechnics*, vol. 38, iss. 2, Nov. 2012. [Online]. doi:10.1002.prep.201200102

[13] G. B. Schaffer, B. J. Hall, "The influence of the atmosphere on the sintering of aluminum," *Metallurgical and Materials Transactions*, vol. 33A, Oct. 2002.

# INITIAL DISTRIBUTION LIST

1. Defense Technical Information Center
   Ft. Belvoir, Virginia

2. Dudley Knox Library
   Naval Postgraduate School
   Monterey, California